

Article

Antitumor Effects of Poplar Propolis on DLBCL SU-DHL-2 Cells

Xiaoqing Liu ^{1,2,†}, Yuanyuan Tian ^{1,2,†}, Ao Yang ^{1,2}, Chuang Zhang ^{1,2}, Xiaoqing Miao ² and Wenchao Yang ^{1,2,*}

¹ College of Animal Science (College of Bee Science), Fujian Agriculture and Forestry University, Fuzhou 350002, China

² Bee Product Processing and Application Research Center of the Ministry of Education, Fuzhou 350002, China

* Correspondence: 000q061005@fafu.edu.cn

† These authors contributed equally to this work.

Abstract: Propolis is resinous natural product produced by Western honeybees using beeswax and plant and bud exudates, which has a wide range of biological activities, including antioxidation, antibacterial, anti-inflammation, immune regulation, antitumor, and so on. Diffuse large B-cell lymphoma (DLBCL) is an aggressive cancer, and accounts for about 30% of all lymphomas. The effect of poplar propolis on DLBCL has not been reported. The IC₅₀ of propolis on the proliferation of DLBCL SU-DHL-2 cell line and its proteins and gene expressions were detected by CCK-8 kit, label-free proteomic, and RT-PCR. The results showed that the IC₅₀ of propolis at the 5 × 10⁵/mL cell for 24 h was 5.729 µg/mL. Label-free-based proteomics analysis showed that there were 115 differentially expressed proteins (61 up-regulated and 54 down-regulated proteins) between IC₅₀ dose-treated and solvent control groups. There were 32.47% differential proteins located in the nucleus, 20.78% in the cytoplasm, and 14.29% in mitochondria. The most significant different pathway (*p* = 0.0016) of protein enrichment was ferroptosis (including glutamate–cysteine ligase regulatory subunit, ferritin, and heme oxygenase). The relative expression trend of 17 of the total 22 genes selected according to proteomics results was in line with their encoded protein. The highest protein–protein interaction was serine/threonine-protein kinase PLK, which interacted with 16 differential proteins. In conclusion, poplar propolis inhibited SU-DHL-2 cells via ferroptosis pathway, accelerating cell death and down-regulated serine/threonine-protein kinase PLK1, affecting apoptosis of cell. This result provides a theoretical basis for the treatment of DLBCL using propolis.

Keywords: propolis; diffuse large B-cell lymphoma; SU-DHL-2 cell line; proteomics; ferroptosis



Citation: Liu, X.; Tian, Y.; Yang, A.; Zhang, C.; Miao, X.; Yang, W.

Antitumor Effects of Poplar Propolis on DLBCL SU-DHL-2 Cells. *Foods* **2023**, *12*, 283. <https://doi.org/10.3390/foods12020283>

Academic Editor: Paweł Kafarski

Received: 19 November 2022

Revised: 27 December 2022

Accepted: 2 January 2023

Published: 7 January 2023



Copyright: © 2023 by the authors. Licensee MDPI, Basel, Switzerland. This article is an open access article distributed under the terms and conditions of the Creative Commons Attribution (CC BY) license (<https://creativecommons.org/licenses/by/4.0/>).

1. Introduction

Propolis, a kind of colloidal solid with an aromatic smell, is processed by Western honey bees after collecting resin from plant or tree and mixing with the secretions of their maxillary glands and wax glands. At present, more than 800 compounds have been isolated and extracted from propolis, and most of them are secondary plant metabolites [1]. Its chemical composition is mainly composed of resin (70%), wax (10%), volatile substances (1%), and other organic compounds, including phenolic compounds, esters, flavonoids, terpenes, beta steroids, aromatic aldehydes, alcohols, vitamins, such as vitamins B1, B2, B6, C, and E, minerals, such as magnesium, calcium, potassium, sodium, copper, zinc, manganese, and iron, and enzymes, such as succinate dehydrogenase, glucose-6-phosphatase, adenosine triphosphatase, and acid phosphatase [1–3]. However, different propolis have different chemical compositions depending on its plant origin, regions, and age [3]. Propolis has a wide range of biological activities, such as antibacterial, anti-inflammatory, antioxidant, antitumor, and immune regulation, and has been used in many fields, including food, functional food, medicine and cosmetics, etc. [4].

Among these activities of propolis or its component, antitumor activity, including cancer cell from colorectal, lung, breast, melanoma, gastric, lymphoma, and tongue [5–16], is one of the most important biological properties. It was reported that red propolis

could reduce pre-tumor lesions, the level of oxidative stress, and the number of abnormal crypt lesions, thereby protecting the colon of rats [5]. The combination of propolis and 5-fluorouracil decreases Cox-2, iNOS contents and reduced the number of abnormal crypt foci and pathological lesions in BALB-c mice [6]. Propolis also has selective cytotoxic effects on human lung cancer cells [7] and tumor cells [8]. Propolis (from India) has an antitumor effect against Dalton's lymphoma-bearing mice [9]. Some components in propolis have antitumor activity. Pinobanksin and some of its ester derivatives in propolis inhibit the B-cell lymphoma cell (M12.C3.F6) [10]. Galangin, a common flavonoid in propolis, significantly induced melanoma cell apoptosis and inhibited melanoma cells in vitro [11]. Caffeic acid phenethyl ester (CAPE) and artemillin C in propolis played an antitumor function on carcinoma, malignant melanoma, colorectal adenocarcinoma, liver, lymphoma, and neurofibromatosis cancer cells [12–16]. Artemillin C indirectly killed human and murine malignant tumor cells in vitro and in vivo by activating the immune system [12] and inhibited the proliferation of human colon cancer cells via inducing G0/G1 cell cycle prolongation [13]. It also inhibited the growth of mouse nerve fiber xenografts by blocking the PAK1 signaling pathway [14]. CAPE completely inhibited the DNA replication of breast cancer cells at a concentration of 10 µg/mL [15]. CAPE demonstrated antitumor activity on cutaneous T-cell lymphoma by modulating the expression level of key transcription factors [16]. The antitumor effect of polar propolis against diffuse large B cell lymphoma was not yet reported.

Diffuse large B cell lymphoma (DLBCL) represents approximately 30–40% of all cases in different geographic regions, and the most common type of non-Hodgkin lymphoma worldwide. According to the different gene expression profiles, DLBCL can be divided into germinal center B-cell and non-germinal center B-cell types [17]. Approximately 60–70% of patients were cured with the standard therapy, which is rituximab plus cyclophosphamide, doxorubicin, vincristine, and prednisone (R-CHOP) [18]. Kinds of tumor suppressors had inhibition effects on DLBCL. Fbw7, a substrate recognition element of the evolutionarily conserved SCF-type ubiquitin ligase complex, mediates apoptosis through targeting Stat3 for ubiquitylation and degradation in activated B-cell (ABC)-like subtype DLBCL [19]. B-AP15 inhibits cell migration and induces apoptosis in germinal center B-cell-like (GCB) and ABC-DLBCL cells [20]. Realgar, a Chinese traditional medicine, inhibits DLBCL cell growth and induces cell apoptosis mainly by up-regulation of Caspase-3 and BAX expression and down-regulation of BCL-2 expression [21]. Apoptosis in DLBCL SU-DHL-4 cells was induced by 17-dimethylaminoethylamino-17-demethoxygeldanamycin, which can induce oxidative stress and then inhibit the expression of HSPA5 and Bcl-2 but promote the expression of Bax [22]. Overexpression of miR-195 caused the down-regulation of *IL-10*, *PD-1+T*, and *PD-L1* and increased the secretion of IFN-γ and TNF-α [23]. Although many studies have been carried out on the antitumor activity of propolis on kinds of cancer cells, the study of propolis from China on diffuse large B-cell lymphoma cells has not been reported yet. This study aimed to investigate the effect of propolis on the SU-DHL-2 cells in vitro. Cell proliferation, apoptosis, changes in protein expression, the related gene expression trends, and conduction pathway were determined.

2. Materials and Methods

2.1. Propolis Extraction and Components Determination

Crude poplar propolis was harvested in Qinglong Manchu Autonomous County, Qinhuangdao, Hebei, China. The extraction of crude propolis and its components determination were performed as in our previous report [24]. Briefly, raw propolis was extracted using ethanol (ratio (w/v) of propolis and 70 ethanol was 1:7.5) under the assistance of ultrasonic wave (of 40 kHz, 20 min, and 60 °C for 3 times) and soaking at room temperature for 2 days. The supernatant was partially evaporated under low pressure after centrifuge (4000× g for 10 min). Then, the extract was stored at 4 °C to solidify and remove beeswax on the surface.

2.2. Determination of IC_{50} of Propolis Extract on SU-DHL-2 Cell

SU-DHL-2 cell (ATCC CRL-2956, purchased from Cellcook, Guangzhou, China) was cultured with the medium composed of 89% the modified RPMI-1640 basal medium (purchased from Wuhan Prosper Life Technology Co., Ltd. Wuhan, China), 10% fetal bovine serum (purchased from Cellmax Bio Co., Ltd. Lanzhou, China), and 1% penicillin and streptomycin mixture (purchased from HyClone Biochemical Products Co., Ltd. Shanghai, China) in a 5% CO_2 humidified incubator at 37 °C (C150, Binder, Tuttlingen, German).

Propolis extract was dissolved in DMSO at a concentration of 2 mg/mL. Propolis solution was diluted with a complete medium for 100, 50, 25, 12.5, 6.25, 5, and 2 μ g/mL. A complete medium added DMSO (0.25%, V/V; equal to DMSO in 100 μ g/mL propolis group) was designed as a negative control. They were used to culture SU-DHL-2 cells at a beginning concentration of 5×10^5 cells/mL. Then, the cell suspensions were collected after 24 h to determine cell viability by CCK8 kit (Purchased from DOJINDO, Kumamoto, Japan) at 450 nm using a microplate reader (1510, Thermo Fisher Waltham, MA, USA). IC_{50} of propolis extract on SU-DHL-2 cell for 24 h was calculated using Graphpad Prism 8.4.3 for Windows (GraphPad Software, Inc., La Jolla, CA, USA).

2.3. Different Proteins of Different Group Cells by Proteomics

Cells were cultured with IC_{50} propolis (5.729 μ g/mL) and solvent control (0.143 μ L/mL DMSO in complete medium) at the same condition. After cultivation for 24 h, the cells were collected and snap frozen in liquid nitrogen, and then stored at -80 °C. Their total proteins were extracted according to the references [25,26]. The concentration of total proteins was determined by Coomassie brilliant blue staining [27]. The spectra of proteins in SU-DHL-2 cells were determined using LC-MS-MS with a Q Exactive HF-X mass spectrometer (Thermo Fisher) with a Nanospray Flex™ electrospray ionization (ESI) source by Novgene Biotech Co., Ltd., Beijing, China.

2.4. Detection of Relative Gene Expression

The gene expressions coded key proteins in protein interactions in the ferroptosis pathway and cell cycle (GCL, HO-1, FTH1, HSP70, p62, PPP4R3C, BUB1B, Cyclin B, PLK1) and randomly selected differential proteins (including 9 up-regulated proteins: POLG2, UGDH, NQO1, PPP1CC, TNFRSF10B, ALG8, NADK2, TANK, NDUFS3, and 4 down-regulated proteins: RASSF6, TK1, VNN3, CTU1) were determined using RT-PCR technology. The β -actin was used as the internal reference gene, and primers were designed via NCBI's free online primer design platform. The primer sequences were listed in Supplementary Table S1. The RT-PCR procedure was performed as per our previous report [24] using Real-Time PCR detection by C1000 Touch Thermal Cycler (BIORAD).

2.5. ROS Staining

Total intracellular ROS was determined by staining cells with dichlorofluorescein diacetate using the Reactive Oxygen Species Assay Kit (Beyotime Biotechnology) [28]. Staining of cells was observed and taken photograph under an inverted fluorescence microscope (TS-100f, Nikon).

2.6. Statistical Analysis

All experiments were performed in triplicate. The experimental results were analyzed using Graphpad Prism 8.4.3 for Windows (GraphPad Software, Inc. San Diego, CA, USA) and expressed as mean \pm standard error. Percentages (p) were transformed to arcsin (degree) values (according to the formula: $\arcsin \sqrt{p}$) prior to ANOVA. One-way ANOVA analysis was used to analyze the significance of differences ($p < 0.01$: extremely statistically significant differences between the treatment group and the control group, $p < 0.05$: statistically significant differences). The relative gene expression was represented by the ratio of expression of a gene in propolis-treated cells to that of control cells [29].

The spectra obtained from LC-MS/MS was searched against the uniprot database by Proteome Discoverer 2.2 (Thermo) with a credibility of more than 99% Peptide Spectrum Matches. The identified protein contains at least 1 unique peptide and false discovery rate is less or equal to 1%. The protein quantitation results were statistically analyzed by T-test using Graphpad Prism 8.0.2 for Windows. The proteins whose quantitation significantly different between experimental and control groups ($p \leq 0.05$ and Fold change (FC) ≥ 2 or $FC \leq 0.5$), were defined as differential proteins. All differential proteins were sent to the Gene Ontology database (<http://www.geneontology.org/> (accessed on 16 November 2022)) to calculate the number of proteins in each term. Hypergeometric test was applied to find GO entries that were the highest significantly enriched in different proteins compared with all protein backgrounds. Kyoto Encyclopedia of Genes and Genomes (KEGG) was employed to analyze the pathway (<http://www.genome.ad.jp/kegg/> (accessed on 16 November 2022)). The protein–protein interactions of differential proteins were performed using the String-db server (<http://string.embl.de/> (accessed on 16 November 2022)), in which the minimum required interaction score was medium confidence (0.500). Then, data exported from string-db were loaded into the Cytoscape software (Version 3.9.1; JAVA: 11.0.6 by AdoptOpenJDK) to beautify the PPI network diagram.

3. Results

3.1. Chemical Composition of Ethanol Extracts of Propolis

There are 51 compounds (Supplementary Table S2) identified from ethanol extracts of propolis (EEP) by UPLC-ESI-MS according to the retention time and secondary mass spectrometry fragmentation of the identified compounds verified through the literature using the same chromatographic and mass spectrometry conditions. Among the 51 identified compounds, there are 31 flavonoids, including luteolin, quercetin, apigenin, breasol kaempferol, etc., 12 phenolic compounds, including p-hydroxybenzoic acid, caffeic acid, p-Hydroxycoumaric acid, isoferulic acid, ferulic acid, etc., 6 kinds of acylated glycerol, and 2 kinds of fatty acid compounds.

3.2. The Inhibition Effects of EEP on SU-DHL-2 Cell

Different concentrations of EEP showed different antitumor effects against SU-DHL-2 cells. The inhibition rate of EEP on SU-DHL-2 cells for 24 h treatment was shown in Figure 1. The IC_{50} of EEP on SU-DHL-2 cells for 24 h was 5.729 $\mu\text{g}/\text{mL}$.

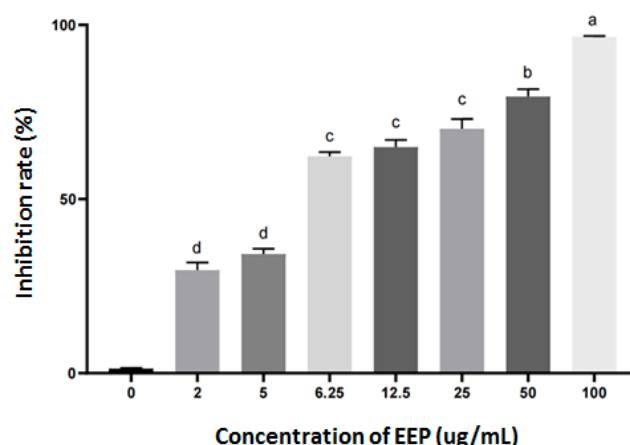


Figure 1. Inhibition rates of SU-DHL-2 cell proliferation by different concentrations of EEP for 24 h. Different letters indicate statistical differences between groups ($p < 0.05$).

3.3. Differential Proteins of SU-DHL-2 Cells Treated by EEP and Control

Differential proteins were screened according to $FC > 2.0$ or $FC < 0.5$ and $p < 0.05$ (EEP vs. control groups). There were 61 up-regulated proteins, and 54 down-regulated proteins

(partly differential proteins ($p < 0.01$) were shown in Supplementary Table S3). Volcano plot of proteins in SU-DHL-2 cells of the two groups was shown in Figure 2.

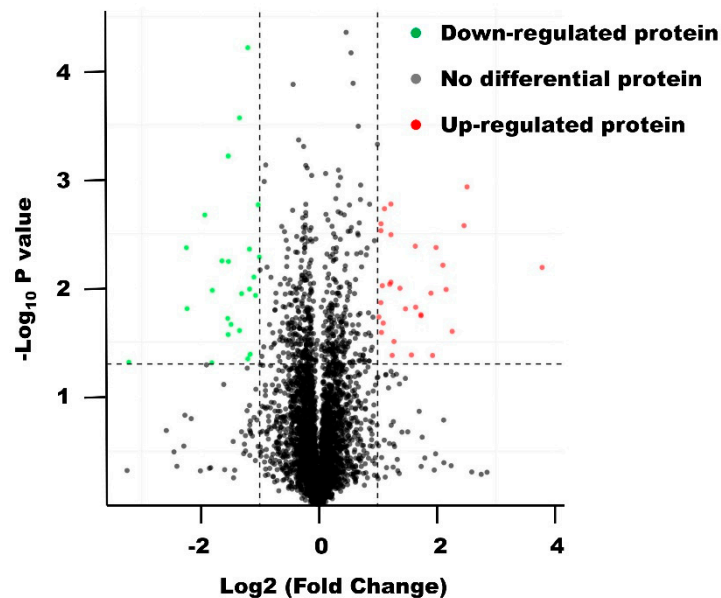


Figure 2. Volcano plot of proteins in SU-DHL-2 cells treated with EEP versus control groups.

The subcellular localization results of the differential proteins showed 32.47% nucleus protein, followed by 20.78% cytoplasm protein, 14.29% mitochondrion protein, 6.49% lysosome proteins, 6.49% endoplasmic reticulum protein, 3.9% plasma membrane protein, 3.90% Golgi apparatus protein, 3.90% extracell protein, 3.90% cytoskeleton protein, 1.30% microsome protein, 1.30% endosome protein, and 1.30% centrosome proteins.

These differential proteins played functions in different pathways. The significant differential proteins in these pathways ($p < 0.05$), which were separately analyzed in up-regulated and down-regulated proteins, were shown in Table 1.

Table 1. These differential proteins in different pathways.

Pathway	<i>p</i> -Value	Description of Proteins
Ferroptosis	0.0016	Glutamate–cysteine ligase regulatory subunit, Ferritin, Heme oxygenase
Mineral absorption	0.0076	Ferritin, Heme oxygenase
Fluid shear stress and atherosclerosis	0.0108	Sequestosome-1, NAD(P)H dehydrogenase [quinone] 1, Heme oxygenase
Ubiquinone and other terpenoid–quinone biosynthesis	0.0247	NAD(P)H dehydrogenase [quinone] 1
Necroptosis	0.0321	Sequestosome-1, Ferritin, Tumor necrosis factor receptor superfamily member 10A DnaJ homolog subfamily C member 3,
Influenza A	0.0414	Epididymis secretory sperm binding protein, Tumor necrosis factor receptor superfamily member 10A
Ubiquitin-mediated proteolysis	0.0431	NEDD8-conjugating enzyme UBE2F, Ubiquitin-conjugating enzyme E2 J1, cDNA, FLJ92255, highly similar to Homo sapiens ring finger protein 7 (RNF7), mRNA

Table 1. Cont.

Pathway	p-Value	Description of Proteins
Ascorbate and aldarate metabolism	0.0488	UDP-glucose 6-dehydrogenase
Antigen processing and presentation	0.0491	Epididymis secretory sperm binding protein, cDNA FLJ78235
Cell cycle	0.0201	Mitotic checkpoint serine/threonine-protein kinase BUB1 beta, Serine/threonine-protein kinase PLK, G2/mitotic-specific cyclin-B2
Progesterone-mediated oocyte maturation	0.0387	Serine/threonine-protein kinase PLK, G2/mitotic-specific cyclin-B2
FoxO signaling pathway	0.0430	Serine/threonine-protein kinase PLK, G2/mitotic-specific cyclin-B2
Hippo signaling pathway—multiple species	0.0457	Ras association domain-containing protein 6

All the interactions of differential proteins were shown in Figure 3. Among the interactions of up-regulated proteins, heat shock protein 70 (HSP70) was the most interacted protein with 13 proteins. Among the interactions of down-regulated proteins, serine/threonine-protein kinase PLK (PLK1 or PLK) was the most interacted protein with 16 differential proteins.

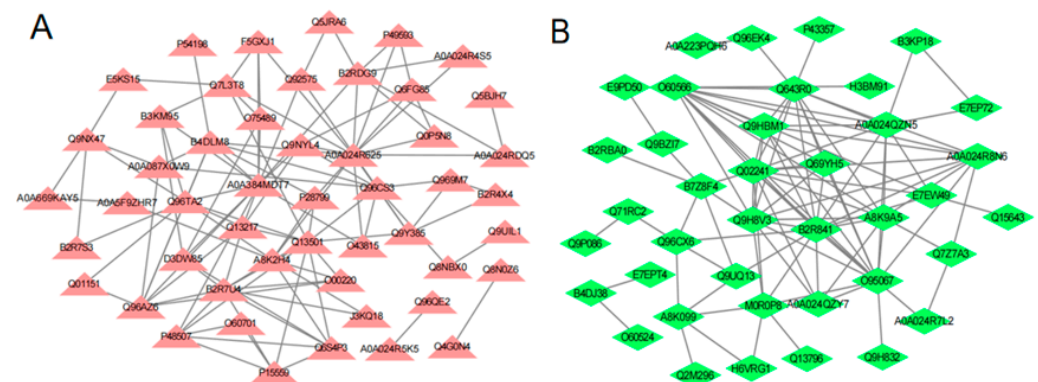


Figure 3. Interaction of differential proteins: (A) interaction diagram of differentially up-regulated proteins; (B) interaction diagram of differentially down-regulated proteins. The triangles or diamonds represent proteins, straight lines represent the interaction relationship between proteins.

3.4. RT-PCR Identification

The results of relative gene expression were shown in Figure 4. The expressions of *GCLC*, *HO-1*, *PPP4R3C*, and *FTH1* were up-regulated; the relative expressions of *BUB1B*, *Cyclin B*, and *PLK1* were down-regulated. They are consistent with the protein expression trend with exception of *p62* and *HSP70* genes. The relative expression of *POLG2*, *UGDH*, *NQO1*, *PPP1CC*, *TNFRSF10B*, *ALG8*, and *NADK2* were up-regulated, and that of *RASSF6*, *TK1*, and *VNN3* were down-regulated. These gene expressions trends were consistent with the coded protein expressions trends with exception of *HSP70*, *NDUFS3*, and *CTU3* genes.

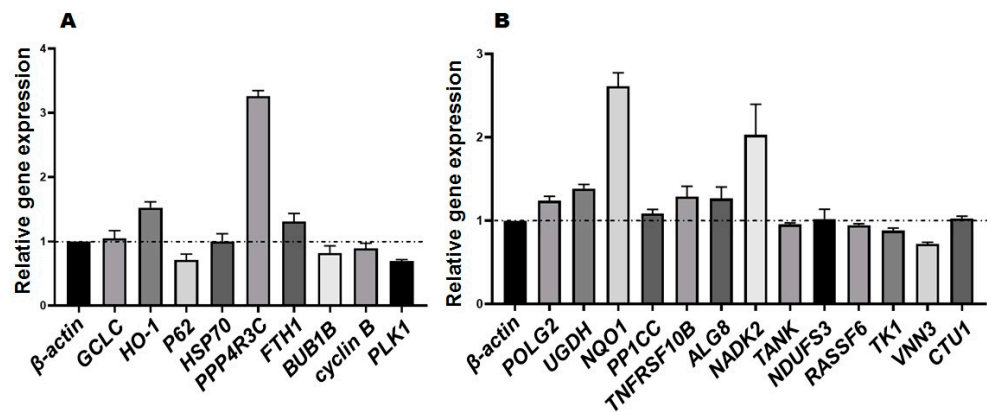


Figure 4. Relative gene expression: (A) genes coded differential proteins screened from ferroptosis pathway, cell cycle pathway and protein interaction; (B) genes coded differential proteins were randomly selected. Genes with expression greater than 1 were up-regulated and less than 1 were down-regulated.

3.5. ROS Staining of SU-DHL-2 Cell

The results showed that the cells treated with EEP have more ROS activity than that of control cell. The photographs of ROS-stained cell are shown in Figure 5.

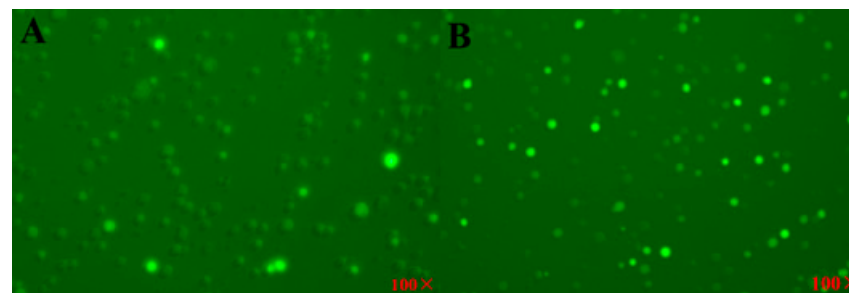


Figure 5. ROS staining of SU-DHL-2 cells: (A) control group; (B) treatment group, propolis at IC₅₀ ($\times 100$).

4. Discussion

Among the 51 identified compounds of EEP, there are 31 flavonoids, including luteolin, quercetin, apigenin, breasol kaempferol, etc., 12 phenolic compounds, including p-hydroxybenzoic acid, caffeic acid, p-Hydroxycoumaric acid, isoferulic acid, ferulic acid, etc., 6 kinds of acylated glycerol, and 2 kinds of fatty acid compounds. The components of EEP used in this experiment were more than others, which were 20 components [30], 31 components [31], 49 components [24] in EEP (poplar) harvested in Yunnan, Shandong, and Shandong, China, respectively. These differences in chemicals and quantities were caused by the region, plant source, and age of propolis [32].

Different propolis have different antitumor activities. It was reported that EEP from three different sources had selective cytotoxicity, and the IC₅₀ on tongue cancer cells treated for 24 h were about 88 $\mu\text{g}/\text{mL}$, 110 $\mu\text{g}/\text{mL}$, and 150 $\mu\text{g}/\text{mL}$, respectively [33]. The IC₅₀ of propolis extract (nano-vesicular formulation of propolis) on A549 lung cancer and BEAS-2B healthy lung cells were $25.44 \pm 4.97 \mu\text{g}/\text{mL}$ and $55.68 \pm 6.24 \mu\text{g}/\text{mL}$ [34]. The IC₅₀ of EEP samples from different regions in Thailand against A549 cells were $106 \pm 0.004 \mu\text{g}/\text{mL}$, $199 \pm 0.009 \mu\text{g}/\text{mL}$, and $87 \pm 0.012 \mu\text{g}/\text{mL}$, and for HeLa cells were $81 \pm 0.006 \mu\text{g}/\text{mL}$, $116 \pm 0.023 \mu\text{g}$, and $54 \pm 0.005 \mu\text{g}/\text{mL}$, respectively [35]. The IC₅₀ of hydroalcoholic Brazilian red propolis on Hep-2 cells was $145.40 \pm 6.56 \mu\text{g}/\text{mL}$ after treatment for 24 h on Hep-2 cells [36]. Chinese propolis water extract and its effective components induced apoptosis of breast cancer cells (MCF-7, MDA-MB-231, A549, and HeLa cells) by inhibiting tumor cell migration, activating caspase 3, and promoting ROS production when the

concentrations of propolis and each of its effective components (pinobanksin, caffeic acid benzyl ester, caffeic acid phenethyl ester, apigenin, pinocembrin, chrysin, and galangin) were 100 µg/mL and 80 µM [37]. Massive apoptosis was found in human lymphocytic leukemia cells treated with 10 µM CAPE [38]. The IC₅₀ of EEP against SU-DHL-2 cells was 5.729 µg/mL (Figure 1), which is far lower than these reports. Propolis exhibits different cytotoxicity to different tumor cell lines, which may be related to the cell concentration and sensitivity to propolis, extraction method, compounds, and duration of action of propolis.

The antitumor mechanism of propolis varied because of different types of cancers or their cell lines, different plant sources of propolis, and the delivery system of the drug. The proteomic technology was widely used to determine the differential proteins in different treatment cells. There were 115 differential proteins between EEP-treated and control SU-DHL-2 cells, which engaged in different pathways to inhibit the proliferation of the cancer cell (Table 1). The highest significant pathway was ferroptosis ($p = 0.0017$), which was also found in antitumor effects on other cancer cells [39]. This result was identified by the result of ROS staining (Figure 5). The ferroptosis pathway includes differential proteins of glutamate-cysteine ligase regulatory subunit (GCLM), ferritin (FTH1), and heme oxygenase (HO). GCLM might control the glutathione (GSH) levels and increase the efficiency of γ -glutamyl-cysteine synthesis in response to oxidative stress [40]. Then, higher GSH content in cancer cells with the antitumor drugs had higher cell growth inhibition potencies [41]. It was reported that ferritin enhanced apoptosis of non-small cell lung cancer cells through the modulation of the miR-125b/p53 axis [42]. It also had antigrowth effects in breast cancer cells by inhibiting the expression of c-MYC [43] and ovarian cancer stem cells [44]. HO has HO-1, HO-2, and HO-3 isoforms, of which HO-1 and HO-2 catalyze the heme into biliverdin, iron, and carbon monoxide. Overexpression of HO-1 is in response to substrate heme, proinflammatory cytokines, reactive oxygen species (ROS), nitric oxide (NO), metalloporphyrins, heavy metals, prostaglandins, UV irradiation, and others [45]. HO-1 induced ferroptotic cell death of HT-1080 fibrosarcoma cells [46], human breast cancer, and lung cancer cells by mediating BAY 11-7085 [47], human colon cancer cells [48], and eradicated high-risk neuroblastoma [49]. Our results (Table 1) showed that HO-1 in the ferroptosis pathway induced the death of SU-DHL-2 cells treated by EEP. Proteins of ferritin and heme oxygenase were also involved in mineral absorption pathway ($p = 0.0076$), which is a common pathway in antitumor reports, such as colorectal cancer [50], colon cancer cells [51], prostate cancer [52], etc. Heme oxygenase also plays an important antitumor effect in fluid shear stress and atherosclerosis pathway ($p = 0.0108$). Ferritin was also involved in necroptosis pathway ($p = 0.0321$).

Another significant pathway is the fluid shear stress and atherosclerosis and ubiquinone pathway, which includes sequestosome-1, which is also involved in necroptosis pathway ($p = 0.0321$), NAD(P)H dehydrogenase [quinone] 1, and heme oxygenase. Sequestosome-1, which is also called p62, is a multidomain, multifunctional protein, which is involved in autophagy, defense against oxidative stress via activation of the Keap1/Nrf2 system, protein aggregation and sequestration, and apoptosis for different types of cancer cells [53–55]. NAD(P)H dehydrogenase [quinone] 1 was also involved in Ubiquinone and other terpenoid-quinone biosynthesis pathways ($p = 0.0247$). This NAD(P)H quinone dehydrogenase 1 could maintain p53 stability for breast cancer cells [56]. Tumor necrosis factor receptor superfamily member 10A is one of the tumor necrosis factors involved in the necroptosis pathway. It is reported that tumor necrosis factor played an important role in apoptosis in an ovarian cancer cell line [57]. Pathways of influenza A, ubiquitin-mediated proteolysis, ascorbate and aldarate metabolism, and antigen processing and presentation also played an important role in the cancer cell death process.

Apart from the up-regulation pathway, down-regulation pathways of cell cycle, progesterone-mediated oocyte maturation, foxO signaling, hippo signaling pathway—multiple species—also contributed to the antitumor effect of EEP on SU-DHL-2 cells. Cell cycle kinases were designed as targets of therapeutic drug development for cancer [58,59]. Forkhead box O (FoxO), the subfamily of the fork head transcription factor family with

important roles in cell fate decisions, plays a pivotal functional role as a tumor suppressor in a wide range of cancers. Ras association domain-containing protein 6 in the hippo signaling pathway is one of the members of the Ras-association domain family that form the core of a highly conserved tumor suppressor network [60].

Among protein–protein interactions, PLK1 was the most interacted protein. It was reported that the down-regulation of PLK1 induced apoptosis [61], premature senescence [62], and elevation drug sensitivity [63] of breast cancer cells and decreased the viability of cancer cells in endothelial cells [64], cell cycle arrest, and apoptosis of cutaneous T-cell lymphomas [65]. Expression of PLK1-inhibited or siRNA-treated showed antitumor activity against prostate, breast, cervical, colon, and lung cancer cells [66–68], etc. PLK1 has a potential application strategy in cancer therapy [66–69]. Knockdown of *KIF23* or inhibition of *KIF23*, a secondary high interacted protein with 14 proteins, suppressed the growth of lung cancer cells [70,71], triple negative breast cancer cells (MDA-MB-231 and BT549) [72], glioma [73], etc. It was also reported that patients with a high expression of *KIF23* had a poor survival [74]. Hsp70 is a dual-function protein, intracellular Hsp70 suppressed apoptosis and lysosomal cell death, and extracellular Hsp70 promoted tumorigenesis and angiogenesis. Additionally, other evidence showed that intracellular Hsp70 promoted apoptosis, and membrane-associated/extracellular Hsp70 elicited antitumor innate and adaptive immune responses [75]. Other differential proteins also played important roles in the antitumor activity of EEP against SU-DHL-2 cells.

The relative expression trend of genes selected to perform RT-PCR was not absolutely the same as their proteins. Although most autosomal gene replication is carried out at the protein level, the copy-number of 23–33% of proteins in complex proteins were influenced by post-transcriptional regulation [76]. The correlation between protein and mRNA is about 0.5 [77], which is weak for the structurally stable proteins and mRNA expression and relatively poor for less stable mRNA and protein expression in high-grade serous ovarian cancer [78]. It was also reported that about 30% of mRNA transcription is not related to protein expression in breast cancer [79].

There are some defects in this antitumor research using cell line, but the xenograft in nude mice did not succeed many times. This may be caused by fewer cancer stem cells in the SU-DHL-2 cell samples injected in nude mice. The metabonomics, cancer stem cell or xenograft model, deletion genes of key proteins, or other methods can be employed to explore more accurate regulation of EPP antitumor against the SU-DHL-2 cell approach for new drug development.

5. Conclusions

The IC_{50} of propolis at the 5×10^5 /mL cell for 24 h was 5.729 μ g/mL. Its antitumor mechanism was explored by label-free-based proteomics, which showed that there were 115 differentially expressed proteins between IC_{50} treated and solvent control groups, which were 61 up-regulated (53.04%) and 54 down-regulated (46.96%) proteins. The main pathway of protein enrichment was the ferroptosis pathway. The most interacted protein was serine/threonine-protein kinase PLK, which interacted with 16 differential proteins. In conclusion, poplar propolis inhibited SU-DHL-2 cells via ferroptosis pathway, accelerating cell death, and down-regulated serine/threonine-protein kinase PLK, affecting apoptosis of the cell.

Supplementary Materials: The following supporting information can be downloaded at: <https://www.mdpi.com/article/10.3390/foods12020283/s1>, Table S1: Primers sequence for RT-PCR. Table S2: Components of EEP. Table S3: Partly differential proteins ($p < 0.01$). Refs. [80–83] cited in Supplementary Materials.

Author Contributions: Conceptualization, X.M. and W.Y.; methodology, W.Y.; data curation, X.L., Y.T. and C.Z.; formal analysis, X.L. and A.Y.; writing—original draft preparation, Y.T. and X.L.; writing—review and editing, W.Y.; supervision, W.Y. All authors have read and agreed to the published version of the manuscript.

Funding: This research received no external funding.

Data Availability Statement: Data are contained within this article.

Acknowledgments: Thanks for the help from Xin Lin during performance of the protocol.

Conflicts of Interest: The authors declare no conflict of interest.

References

1. Kasote, D.; Bankova, V.; Viljoen, A.M. Propolis: Chemical diversity and challenges in quality control. *Phytochem. Rev.* **2022**, *21*, 1887–1911. [[CrossRef](#)] [[PubMed](#)]
2. Salatino, A.; Salatino, M.L.F. Scientific note: Often quoted, but not factual data about propolis composition. *Apidologie* **2021**, *52*, 312–314. [[CrossRef](#)]
3. Šturm, L.; Ulrih, N.P. Advances in the propolis chemical composition between 2013 and 2018: A review. *eFood* **2020**, *1*, 24–37. [[CrossRef](#)]
4. El-Guendouz, S.; Lyoussi, B.; Miguel, M.G. Insight on propolis from mediterranean countries: Chemical composition, biological activities and application fields. *Chem. Biodivers* **2019**, *16*, e1900094. [[CrossRef](#)] [[PubMed](#)]
5. Braga, V.N.L.; Juanes, C.D.C.; Peres, H.D.S.; Sousa, J.R.D.; Cavalcanti, B.C.; Jamaru, F.V.F.; de Lemos, T.L.G.; Dornelas, C.A. Gum arabic and red propolis protect colorectal preneoplastic lesions in a rat model of azoxymethane. *Acta Cir. Bras.* **2019**, *34*, e201900207. [[CrossRef](#)] [[PubMed](#)]
6. Sameni, H.R.; Yosefi, S.; Alipour, M.; Pakdel, A.; Torabizadeh, N.; Semnani, V.; Bandegi, A.R. Co-administration of 5FU and propolis on AOM/DSS induced colorectal cancer in BALB-c mice. *Life Sci.* **2021**, *276*, 119390. [[CrossRef](#)]
7. Demir, S.; Aliyazicioglu, Y.; Turan, I.; Misir, S.; Mentese, A.; Yaman, S.O.; Akbulut, K.; Deger, O. Antiproliferative and proapoptotic activity of Turkish propolis on human lung cancer cell line. *Nutr. Cancer* **2016**, *68*, 165–172. [[CrossRef](#)]
8. Xuan, H.; Li, Z.; Yan, H.; Sang, Q.; Wang, K.; He, Q.; Wang, Y.; Hu, F. Antitumor activity of Chinese propolis in human breast cancer MCF-7 and MDA-MB-231 Cells. *Evid-Based Compl. Alt.* **2014**, *2014*, e280120. [[CrossRef](#)]
9. Prasad, S.B.; Turnia, I. Antitumor activity with no toxicity of propolis from Meghalaya, India in ascites Dalton's lymphoma-bearing mice. *Indian J. Nat. Prod. Resour.* **2021**, *11*, 267–279. [[CrossRef](#)]
10. Alday, E.; Valencia, D.; Carreño, A.; Picerno, P.; Piccinelli, A.L.; Rastrelli, L.; Robles-Zepeda, R.; Hernandez, J.; Velazquez, C. Apoptotic induction by pinobanksin and some of its ester derivatives from Sonoran propolis in a B-cell lymphoma cell line. *Chem.-Biol. Interact.* **2015**, *242*, 35–44. [[CrossRef](#)]
11. Benguedouar, L.; Lahouel, M.; Gangloff, S.; Durlach, A.; Grange, F.; Bernard, P.; Antonicelli, F. Algerian ethanolic extract of propolis and galangin decreased melanoma tumour progression in C57BL6 mice. *Ann. Dermatol. Syphiligr.* **2015**, *142*, S294. [[CrossRef](#)]
12. Kimoto, T.; Arai, S.; Kohguchi, M.; Aga, M.; Nomura, Y.; Micallef, M.J.; Kurimoto, M.; Mito, K. Apoptosis and suppression of tumor growth by artemillin C extracted from Brazilian propolis. *Cancer Detect. Prev.* **1998**, *22*, 506–515. [[CrossRef](#)] [[PubMed](#)]
13. Shimizu, K.; Ashida, H.; Matsuura, Y.; Kanazawa, K. Antioxidative bioavailability of artemillin C in Brazilian propolis. *Arch. Biochem. Biophys.* **2004**, *424*, 181–188. [[CrossRef](#)] [[PubMed](#)]
14. Messerli, S.M.; Ahn, M.R.; Kunimasa, K.; Yanagihara, M.; Tatefuji, T.; Hashimoto, K.; Mautner, V.; Uto, Y.; Hori, H.; Kumazawa, S.; et al. Artemillin C (ARC) in Brazilian green propolis selectively blocks oncogenic PAK1 signaling and suppresses the growth of NF tumors in mice. *Phytother. Res.* **2009**, *23*, 423–427. [[CrossRef](#)]
15. Grunberger, D.; Banerjee, R.; Eisinger, K.; Oltz, E.M.; Efros, L.; Caldwell, M.; Estevez, V.; Nakanishi, K. Preferential cytotoxicity on tumor cells by caffeic acid phenethyl ester isolated from propolis. *Experientia* **1988**, *44*, 230–232. [[CrossRef](#)]
16. Jayakumar, A.; Venugopal, R.; Zielinski, R.; Rusin, A.; Fokt, I.; Skora, S.; Ni, X.; Duvis, M.; Priebe, W. High sensitivity of cutaneous T-cell lymphoma (CTCL) to CAFE, a component of propolis. *Cancer Res.* **2015**, *75*, 2096. [[CrossRef](#)]
17. Arber, D.A.; Orazi, A.; Hasserjian, R.; Thiele, J.; Borowitz, M.J.; Le Beau, M.M.; Bloomfield, C.D.; Cazzola, M.; Vardiman, J.W. The 2016 revision of the World Health Organization classification of lymphoid neoplasms. *Blood* **2016**, *127*, 2391–2405. [[CrossRef](#)]
18. Li, S.; Young, K.H.; Medeiros, L.J. Diffuse large B-cell lymphoma. *Pathology* **2018**, *50*, 74–87. [[CrossRef](#)]
19. Yao, S.; Xu, F.; Chen, Y.; Ge, Y.; Zhang, F.; Huang, H.; Li, L.; Lin, D.; Luo, X.; Xu, J.; et al. Fbw7 regulates apoptosis in activated B-cell like diffuse large B-cell lymphoma by targeting Stat3 for ubiquitylation and degradation. *J. Exp. Clin. Cancer Res.* **2017**, *36*, e10. [[CrossRef](#)]
20. Jiang, L.; Sun, Y.; Wang, J.; He, Q.; Chen, X.; Lan, X.; Chen, J.; Dou, Q.; Shi, X.; Liu, J. Proteasomal cysteine deubiquitinase inhibitor b-AP15 suppresses migration and induces apoptosis in diffuse large B cell lymphoma. *J. Exp. Clin. Cancer Res.* **2019**, *38*, 1756–1766. [[CrossRef](#)]
21. Shi, L.; Zhu, H.; Zhang, M.; Liu, Y.; Wang, Y.; Zhao, J.; Lei, F.; He, P. Effect of realgar on induction of apoptosis in DLBCL cell line SU-DHL-4 and its possible mechanisms. *J. Exp. Hematol.* **2014**, *22*, 729–734. [[CrossRef](#)]
22. Li, J.; Zhang, J.; Wang, X.; Sun, Z. Effects of 17-DMAG on diffuse large B-cell lymphoma cell apoptosis. *Exp. Ther. Med.* **2017**, *14*, 3727–3731. [[CrossRef](#)] [[PubMed](#)]
23. He, B.; Yan, F.; Wu, C. Overexpressed miR-195 attenuated immune escape of diffuse large B-cell lymphoma by targeting PD-L1. *Biomed. Pharmacother.* **2018**, *98*, 95–101. [[CrossRef](#)] [[PubMed](#)]

24. Xu, X.; Pu, R.; Li, Y.; Wu, Z.; Li, C.; Miao, X.; Yang, W. Chemical compositions of propolis from China and the United States and their antimicrobial activities against *Penicillium notatum*. *Molecules* **2019**, *24*, 3576. [[CrossRef](#)] [[PubMed](#)]
25. Kachuk, C.; Stephen, K.; Doucette, A. Comparison of sodium dodecyl sulfate depletion techniques for proteome analysis by mass spectrometry. *J. Chromatogr. A* **2015**, *1418*, 158–166. [[CrossRef](#)]
26. Wiśniewski, J.R.; Zougman, A.; Nagaraj, N.; Mann, M. Universal sample preparation method for proteome analysis. *Nat. Methods* **2009**, *6*, 359–362. [[CrossRef](#)]
27. Noaman, N.; Coorssen, J.R. Coomassie does it (better): A Robin Hood approach to total protein quantification. *Anal. Biochem.* **2018**, *556*, 53–56. [[CrossRef](#)]
28. Liu, M.; Jin, L.; Sun, S.; Liu, P.; Feng, X.; Cheng, Z.; Liu, W.; Guan, K.; Shi, Y.; Yuan, H. Metabolic reprogramming by PCK1 promotes TCA cataplerosis, oxidative stress and apoptosis in liver cancer cells and suppresses hepatocellular carcinoma. *Oncogene* **2018**, *37*, 1637–1653. [[CrossRef](#)]
29. Livak, K.J.; Schmittgen, T.D. Analysis of relative gene expression data using real-time quantitative PCR and the 2[−]ΔΔCT Method. *Methods* **2001**, *25*, 402–408. [[CrossRef](#)]
30. Sun, Y.; Rao, G. Studies on chemical constituents of Yunnan propolis. *J. Chin. Med. Mater.* **2016**, *39*, 2247–2250. [[CrossRef](#)]
31. Yao, J.; Sun, J.; Wu, L.; Wang, H.; Wang, G.; Ye, W. Identification of major constituents from propolis by LC-IT-TOF-MS. *J. China Pharm. Univ.* **2017**, *48*, 178–183. [[CrossRef](#)]
32. de Groot, A.C. Propolis: A review of properties, applications, chemical composition, contact allergy, and other adverse effects. *Dermatitis* **2013**, *24*, 263–282. [[CrossRef](#)] [[PubMed](#)]
33. Wezgowiec, J.; Wieczynska, A.; Wieckiewicz, W.; Kulbacka, J.; Saczko, J.; Pachura, N.; Wieckiewicz, M.; Gancarz, R.; Wilk, K.A. Polish propolis-chemical composition and biological effects in tongue cancer cells and macrophages. *Molecules* **2020**, *25*, 2426. [[CrossRef](#)] [[PubMed](#)]
34. Ilhan-Ayisigi, E.; Ulucan, F.; Saygili, E.; Saglam-Metiner, P.; Gulce-Iz, S.; Yesil-Celiktas, O. Nano-vesicular formulation of propolis and cytotoxic effects in a 3D spheroid model of lung cancer. *J. Sci. Food Agric.* **2020**, *100*, 3525–3535. [[CrossRef](#)] [[PubMed](#)]
35. Khacha-Ananda, S.; Tragoolpua, K.; Chantawannakul, P.; Tragoolpua, Y. Propolis extracts from the northern region of Thailand suppress cancer cell growth through induction of apoptosis pathways. *Investig. New Drugs* **2016**, *34*, 707–722. [[CrossRef](#)]
36. da Silva Frozza, C.O.; Santos, D.A.; Rufatto, L.C.; Minetto, L.; Scariot, F.J.; Echeverrigaray, S.; Pich, C.T.; Moura, S.; Padilha, F.F.; Borsuk, S. Antitumor activity of Brazilian red propolis fractions against Hep-2 cancer cell line. *Biomed. Pharmacother.* **2017**, *91*, 951–963. [[CrossRef](#)]
37. Xuan, H.; Wang, Y.; Li, A.; Fu, C.; Wang, Y.; Peng, W. Bioactive components of Chinese propolis water extract on antitumor activity and quality control. *Evid-Based Compl. Alt.* **2016**, *2016*, 9641965. [[CrossRef](#)]
38. Avci, Ç.B.; Gündüz, C.; Baran, Y.; Şahin, F.; Yılmaz, S.; Dogan, Z.O.; Saydam, G. Caffeic acid phenethyl ester triggers apoptosis through induction of loss of mitochondrial membrane potential in CCRF-CEM cells. *J. Cancer Res. Clin. Oncol.* **2011**, *137*, 41–47. [[CrossRef](#)]
39. Xu, T.; Ding, W.; Ji, X.; Ao, X.; Liu, Y.; Yu, W.; Wang, J. Molecular mechanisms of ferroptosis and its role in cancer therapy. *J. Cell. Mol. Med.* **2019**, *23*, 4900–4912. [[CrossRef](#)]
40. Cortes-Wanstreet, M.M.; Giedzinski, E.; Limoli, C.L.; Luderer, U. Overexpression of glutamate–cysteine ligase protects human COV434 granulosa tumour cells against oxidative and γ-radiation-induced cell death. *Mutagenesis* **2009**, *24*, 211–224. [[CrossRef](#)]
41. Bracht, K.; Grünert, R.; Bednarski, P.J. Correlations between the activities of 19 anti-tumor agents and the intracellular glutathione concentrations in a panel of 14 human cancer cell lines: Comparisons with the National Cancer Institute data. *Anti-Cancer Drugs* **2006**, *17*, 41–51. [[CrossRef](#)] [[PubMed](#)]
42. Biamonte, F.; Battaglia, A.M.; Zolea, F.; Oliveira, D.M.; Aversa, I.; Santamaria, G.; Giovannone, E.D.; Rocco, G.; Viglietto, G.; Costanzo, F. Ferritin heavy subunit enhances apoptosis of non-small cell lung cancer cells through modulation of miR-125b/p53 axis. *Cell Death Dis.* **2018**, *9*, 1174. [[CrossRef](#)] [[PubMed](#)]
43. Ali, A.; Shafarin, J.; Abu Jabal, R.; Aljabi, N.; Hamad, M.; Sualeh Muhammad, J.; Unnikannan, H.; Hamad, M. Ferritin heavy chain (FTH1) exerts significant antigrowth effects in breast cancer cells by inhibiting the expression of c-MYC. *FEBS Open Bio.* **2021**, *11*, 3101–3114. [[CrossRef](#)] [[PubMed](#)]
44. Lobello, N.; Biamonte, F.; Pisanu, M.E.; Faniello, M.C.; Jakopin, Ž.; Chiarella, E.; Giovannone, E.D.; Mancini, R.; Ciliberto, G.; Cuda, G.; et al. Ferritin heavy chain is a negative regulator of ovarian cancer stem cell expansion and epithelial to mesenchymal transition. *Oncotarget* **2016**, *7*, 62019. [[CrossRef](#)] [[PubMed](#)]
45. Podkalicka, P.; Mucha, O.; Józkwicz, A.; Dulak, J.; Łoboda, A. Heme oxygenase inhibition in cancers: Possible tools and targets. *Contemp. Oncol. (Pozn)* **2018**, *22*, 23–32. [[CrossRef](#)]
46. Kwon, M.Y.; Park, E.; Lee, S.J.; Chung, S.W. Heme oxygenase-1 accelerates erastin-induced ferroptotic cell death. *Oncotarget* **2015**, *6*, 24393–24403. [[CrossRef](#)]
47. Chang, L.; Chiang, S.; Chen, S.; Yu, Y.; Chou, R.; Chang, W. Heme oxygenase-1 mediates BAY 11–7085 induced ferroptosis. *Cancer Lett.* **2018**, *416*, 124–137. [[CrossRef](#)]
48. Malfa, G.A.; Tomasello, B.; Acquaviva, R.; Genovese, C.; La Mantia, A.; Cammarata, F.P.; Ragusa, M.; Renis, M.; Di Giacomo, C. *Betula etnensis* Raf. (Betulaceae) extract induced HO-1 expression and ferroptosis cell death in human colon cancer cells. *Int. J. Mol. Sci.* **2019**, *20*, 2723. [[CrossRef](#)] [[PubMed](#)]

49. Fest, S.; Soldati, R.; Christiansen, N.M.; Zenclussen, M.L.; Kilz, J.; Berger, E.; Starke, S.; Lode, H.N.; Engel, C.; Zenclussen, A.C.; et al. Targeting of heme oxygenase-1 as a novel immune regulator of neuroblastoma. *Int. J. Cancer* **2016**, *138*, 2030–2042. [[CrossRef](#)]
50. Yu, C.; Chen, F.; Jiang, J.; Zhang, H.; Zhou, M. Screening key genes and signaling pathways in colorectal cancer by integrated bioinformatics analysis. *Mol. Med. Rep.* **2019**, *20*, 1259–1269. [[CrossRef](#)]
51. Zeng, H.; Lazarova, D.L.; Bordonaro, M. Mechanisms linking dietary fiber, gut microbiota and colon cancer prevention. *World J. Gastrointest Oncol.* **2014**, *6*, 41. [[CrossRef](#)] [[PubMed](#)]
52. He, Z.; Duan, X.; Zeng, G. Identification of potential biomarkers and pivotal biological pathways for prostate cancer using bioinformatics analysis methods. *PeerJ* **2019**, *7*, e7872. [[CrossRef](#)] [[PubMed](#)]
53. Thai, S.F.; Jones, C.P.; Robinette, B.L.; Ren, H.; Vallant, B.; Fisher, A.; Kitchin, K.T. Effects of copper nanoparticles on mRNA and small RNA expression in human hepatocellular carcinoma (HepG2) cells. *J. Nanosci. Nanotechnol.* **2021**, *21*, 5083–5098. [[CrossRef](#)] [[PubMed](#)]
54. Denk, H.; Stumptner, C.; Abuja, P.M.; Zatloukal, K. Sequestosome 1/p62-related pathways as therapeutic targets in hepatocellular carcinoma. *Expert Opin. Ther. Targets* **2019**, *23*, 393–406. [[CrossRef](#)] [[PubMed](#)]
55. Katsuragi, Y.; Ichimura, Y.; Komatsu, M. Regulation of the Keap1–Nrf2 pathway by p62/SQSTM1. *Curr. Opin. Toxicol.* **2016**, *1*, 54–61. [[CrossRef](#)]
56. Patiño-Morales, C.C.; Soto-Reyes, E.; Arechaga-Ocampo, E.; Ortiz-Sánchez, E.; Antonio-Véjar, V.; Pedraza-Chaverri, J.; García-Carrancá, A. Curcumin stabilizes p53 by interaction with NAD (P) H: Quinone oxidoreductase 1 in tumor-derived cell lines. *Redox Biol.* **2020**, *28*, 101320. [[CrossRef](#)]
57. Sheikhshabani, S.H.; Amini-Farsani, Z.; Rahmati, S.; Jazaeri, A.; Mohammadi-Samani, M.; Asgharzade, S. Oleuropein reduces cisplatin resistance in ovarian cancer by targeting apoptotic pathway regulators. *Life Sci.* **2021**, *278*, 119525. [[CrossRef](#)]
58. Pitts, T.M.; Davis, S.L.; Eckhardt, S.G.; Bradshaw-Pierce, E.L. Targeting nuclear kinases in cancer: Development of cell cycle kinase inhibitors. *Pharmacol. Ther.* **2014**, *142*, 258–269. [[CrossRef](#)]
59. Blagden, S.; Bono, J. Drugging cell cycle kinases in cancer therapy. *Curr. Drug Targets* **2005**, *6*, 325–335. [[CrossRef](#)]
60. Mohajan, S.; Jaiswal, P.K.; Vatanmakarian, M.; Yousefi, H.; Sankaralingam, S.; Alahari, S.K.; Alahari, S.K.; Koul, S.; Koul, H.K. Hippo pathway: Regulation, deregulation and potential therapeutic targets in cancer. *Cancer Lett.* **2021**, *507*, 112–123. [[CrossRef](#)]
61. Kang, G.Y.; Lee, E.R.; Kim, J.H.; Jung, J.W.; Lim, J.; Kim, S.K.; CHO, S.G.; Kim, K.P. Downregulation of PLK-1 expression in kaempferol-induced apoptosis of MCF-7 cells. *Eur. J. Pharmacol.* **2009**, *611*, 17–21. [[CrossRef](#)]
62. Dimri, M.; Cho, J.H.; Kang, M.; Dimri, G.P. PLK1 inhibition down-regulates polycomb group protein BMI1 via modulation of the miR-200c/141 cluster. *J. Biol. Chem.* **2015**, *290*, 3033–3044. [[CrossRef](#)] [[PubMed](#)]
63. Spänkuch, B.; Heim, S.; Kurunci-Csacsko, E.; Lindenau, C.; Yuan, J.; Kaufmann, M.; Strebhardt, K. Down-regulation of Polo-like kinase 1 elevates drug sensitivity of breast cancer cells in vitro and in vivo. *Cancer Res.* **2006**, *66*, 5836–5846. [[CrossRef](#)] [[PubMed](#)]
64. Gomes, C.P.; Gomes-da-Silva, L.C.; Ramalho, J.S.; de Lima, M.C.; Simoes, S.; Moreira, J.N. Impact of PLK-1 silencing on endothelial cells and cancer cells of diverse histological origin. *Curr. Gene Ther.* **2013**, *13*, 189–201. [[CrossRef](#)]
65. Nihal, M.; Stutz, N.; Schmit, T.; Ahmad, N.; Wood, G.S. Polo-like kinase 1 (Plk1) is expressed by cutaneous T-cell lymphomas (CTCLs), and its downregulation promotes cell cycle arrest and apoptosis. *Cell Cycle* **2011**, *10*, 1303–1311. [[CrossRef](#)]
66. Shao, C.; Ahmad, N.; Hodges, K.; Kuang, S.; Ratliff, T.; Liu, X. Inhibition of polo-like kinase 1 (Plk1) enhances the antineoplastic activity of metformin in prostate cancer. *J. Biol. Chem.* **2015**, *290*, 2024–2033. [[CrossRef](#)]
67. Spänkuch-Schmitt, B.; Bereiter-Hahn, J.; Kaufmann, M.; Strebhardt, K. Effect of RNA silencing of polo-like kinase-1 (PLK1) on apoptosis and spindle formation in human cancer cells. *J. Natl. Cancer Inst.* **2002**, *94*, 1863–1877. [[CrossRef](#)] [[PubMed](#)]
68. Liu, X.; Erikson, R.L. Polo-like kinase (Plk) 1 depletion induces apoptosis in cancer cells. *Proc. Natl. Acad. Sci. USA* **2003**, *100*, 5789–5794. [[CrossRef](#)]
69. Raab, C.A.; Raab, M.; Becker, S.; Strebhardt, K. Non-mitotic functions of polo-like kinases in cancer cells. *Biochim. Biophys. Acta Rev. Cancer* **2021**, *1875*, 188467. [[CrossRef](#)]
70. Kato, T.; Wada, H.; Patel, P.; Hu, H.P.; Lee, D.; Ujiie, H.; Hirohashi, K.; Nakajima, T.; Sato, M.; Kaji, M.; et al. Overexpression of KIF23 predicts clinical outcome in primary lung cancer patients. *Lung Cancer* **2016**, *92*, 53–61. [[CrossRef](#)]
71. Iltzsche, F.; Simon, K.; Stopp, S.; Patschull, G.; Francke, S.; Wolter, P.; Hauser, S.; Murphy, D.J.; Garcia, P.; Rosenwald, A.; et al. An important role for Myb-MuvB and its target gene KIF23 in a mouse model of lung adenocarcinoma. *Oncogene* **2017**, *36*, 110–121. [[CrossRef](#)] [[PubMed](#)]
72. Jian, W.; Deng, X.; Munankarmy, A.; Borkhuu, O.; Ji, C.; Wang, X.; Zheng, W.; Yu, Y.; Zhou, X.; Fang, L. KIF23 promotes triple negative breast cancer through activating epithelial-mesenchymal transition. *Gland. Surg.* **2021**, *10*, 1941. [[CrossRef](#)] [[PubMed](#)]
73. Takahashi, S.; Fusaki, N.; Ohta, S.; Iwahori, Y.; Iizuka, Y.; Inagawa, K.; Kawakami, Y.; Yoshida, K.; Toda, M. Downregulation of KIF23 suppresses glioma proliferation. *J. Neuro-Oncol.* **2012**, *106*, 519–529. [[CrossRef](#)]
74. Liang, W.; Liu, X.; Huang, H.; Gao, Z.; Li, K. Prognostic significance of KIF23 expression in gastric cancer. *World J. Gastro Oncol.* **2020**, *12*, 1104. [[CrossRef](#)] [[PubMed](#)]
75. Vostakolaei, M.A.; Hatami-Baroogh, L.; Babaei, G.; Molavi, O.; Kordi, S.; Abdolizadeh, J. Hsp70 in cancer: A double agent in the battle between survival and death. *J. Cell. Physiol.* **2021**, *236*, 3420–3444. [[CrossRef](#)]
76. Gonçalves, E.; Fragoulis, A.; Garcia-Alonso, L.; Cramer, T.; Saez-Rodriguez, J.; Beltrao, P. Widespread post-transcriptional attenuation of genomic copy-number variation in cancer. *Cell Syst.* **2017**, *5*, 386–398. [[CrossRef](#)]

77. Akbani, R.; Ng, P.K.S.; Werner, H.M.; Shahmoradgoli, M.; Zhang, F.; Ju, Z.; Liu, W.; Yang, J.; Yoshihara, K.; Li, J.; et al. A pan-cancer proteomic perspective on The Cancer Genome Atlas. *Nat. Commun.* **2014**, *5*, 3887. [[CrossRef](#)]
78. Zhang, H.; Liu, T.; Zhang, Z.; Payne, S.H.; Zhang, B.; McDermott, J.E.; Zhou, J.; Petyuk, V.A.; Chen, L.; Ray, D.; et al. Integrated proteogenomic characterization of human high-grade serous ovarian cancer. *Cell* **2016**, *166*, 755–765. [[CrossRef](#)]
79. Johansson, H.J.; Sociarelli, F.; Vacanti, N.M.; Haugen, M.H.; Zhu, Y.; Siavelis, I.; Fernandez-Woodbridge, A.; Aure, M.R.; Sennblad, B.; Vesterlund, M.; et al. Breast cancer quantitative proteome and proteogenomic landscape. *Nat. Commun.* **2019**, *10*, 1600. [[CrossRef](#)]
80. Falcão, S.I.; Vale, N.; Gomes, P.; Domingues, M.R.; Freire, C.; Cardoso, S.M.; Vilas-Boas, M. Phenolic profiling of Portuguese propolis by LC–MS spectrometry: Uncommon propolis rich in flavonoid glycosides. *Phytochem. Anal.* **2013**, *24*, 309–318.
81. Nagaoka, T.; Banskota, A.H.; Tezuka, Y.; Midorikawa, K.; Matsushige, K.; Kadota, S. Caffeic acid phenethyl ester (CAPE) analogues: Potent nitric oxide inhibitors from the Netherlands propolis. *Biol. Pharm. Bull.* **2003**, *26*, 487–491.
82. Bilikova, K.; Popova, M.; Trusheva, B.; Bankova, V.A. New anti-Paenibacillus larvae substances purified from propolis. *Apidologie* **2013**, *44*, 278–285.
83. Bloor, S.; Catchpole, O.; Mitchell, K.; Webby, R.; Davis, P. Antiproliferative acylated glycerols from New Zealand propolis. *J. Nat. Prod.* **2019**, *82*, 2359–2367.

Disclaimer/Publisher’s Note: The statements, opinions and data contained in all publications are solely those of the individual author(s) and contributor(s) and not of MDPI and/or the editor(s). MDPI and/or the editor(s) disclaim responsibility for any injury to people or property resulting from any ideas, methods, instructions or products referred to in the content.